ICES Journal of Marine Science: Journal du Conseil
July 2009 ; Volume 66 (6) : Pages 1155-1161
http://dx.doi.org/10.1093/icesjms/fsp113

A method for reducing uncertainty in estimates of fish-school frequency response using data from multifrequency and multibeam echosounders

Laurent Berger[1, *], Cyrille Poncelet[1] and Verena M. Trenkel[2]

[1] Ifremer, Département NSE, Centre de Brest, Z. I. Pointe du Diable, BP 70, 29280 Plouzané, France
[2] Ifremer, Département EMH, rue de l'Ile d'Yeu, BP 21105, 44311 Nantes Cedex 03, France

*: Corresponding author : L. Berger : tél: +33 298224700; fax: +33 240374075, email address : laurent.berger@ifremer.fr

Abstract:

Fish schools can be insonified simultaneously with multifrequency echosounders (e.g. Simrad EK60s) and a multibeam echosounder (e.g. Simrad ME70). This paper presents a method for combining these data to improve estimates of the relative frequency response $r(f)$ of fish schools. Values of $r(f)$ are now commonly used to classify echoes in fishery surveys. The data from the roll- and pitch-stabilized, high-resolution ME70 are used to correct beam-width effects in the multifrequency EK60 data. First, knowing the exact position and orientation of the transducers and the position of the vessel, the echoes are placed into a common geographic coordinate system. Then, the EK60 data are rejected if they do not include a significant percentage of the fish school imaged with the multibeam echosounder. Echoes that exceed the overlap threshold are used to estimate the $r(f)$. The proposed method is applied to simulated and actual data for sardine and mackerel schools in the Bay of Biscay to estimate their $r(f)$ values. The results for different overlap thresholds are compared with the results of a different method, one that uses adaptive thresholds on volume-backscattering strength S_v. The proposed method reduces uncertainty in estimates of $r(f)$ for schools with an overlap of greater than 80%, and it outperforms the S_v-thresholding technique.

Keywords: acoustics, pelagic fish, *Sardina pilchardus*, *Scomber scombrus*, species identification

1. Introduction

Multifrequency, single-beam echosounders (e.g. Simrad EK60s) and the echo-integration method (EI) are often used for stock assessments of pelagic species. EI requires species identification of the acoustic targets. Such multifrequency data can be used to identify certain species if the data are collected in a way that minimizes the variability in the measured frequency responses of the fish schools (Korneliussen *et al*., 2008).

Acoustic identification of species is especially difficult in areas where small pelagic fish form small schools, such as in the Bay of Biscay (mean school size < 10 m; Massé, 1996). In such cases, the beam widths and motions of echosounder transducers cause uncertainty (bias and imprecision) in the acoustic measure of school morphology, and result in underestimation of fish density and biomass (Diner, 2001):

Beam width: Using simulations, Diner (2007) demonstrated that the size of small schools is increasingly overestimated and their densities are underestimated with increasing beam width;

Transducer positions and beam-steering angles: Korneliussen *et al*. (2008) analysed the effects of transducer positions on multifrequency sampling volumes and measurements of frequency response. At large ranges, differences in beam-steering angle can cause larger differences in the sampled volumes; and

Transducer motion: Sampling volumes are modulated by translation, because of changes in geographic location; pitch, resulting from rotation about an athwartship axis; roll, because of rotation about an alongship axis; and yaw, because of rotation about a vertical axis. Each type of motion can affect measurements of school morphology.

To improve the resolutions and enlarge the sampling volumes of EK60s, Ifremer and Simrad collaboratively developed the first scientific multibeam echosounder, the ME70 (for details, see Trenkel *et al*., 2008). The ME70 compensates the echo data for transducer motion and has narrower beam widths (3–4°) than the EK60 transducers (typically 7°).

This paper proposes a method that uses the stabilized, high-resolution beams of the ME70 to correct EK60 data for multiples of these sources of uncertainty, which consequently improves the measurements of frequency responses used for species identifications. The efficacy of the proposed method is first evaluated for simulated sardine (*Sardina pilchardus*) and mackerel (*Scomber scombrus*) schools, which are parameterized by school size, depth, fish-to-fish spacing, target strength (*TS*) and relative frequency response $r(f)$; nautical-area backscattering coefficients (s_A) at each measurement frequency, normalized to s_A at a reference frequency. Then, the proposed method is applied to sardine and mackerel data collected in the Bay of Biscay and the resulting $r(f)$ are compared with their unprocessed versions.

2. Methods

The proposed method accounts for uncertainty in estimates of $r(f)$ because of beam width and transducer motion; including position, orientation, and navigation effects. Account is taken of the overlapping sampling volumes of multiple-echosounder beams. To do so, a high-resolution image of a fish school is recorded by the ME70. The matrix of pixels is then spatially indexed, and the percentage of fish-school pixels also observed by each single-beam transducer is quantified. The details of each step are given below.

2.1. Common coordinate system

The data from each transducer, defined in their own coordinate system, are transformed through rotation and translation to a common geographic coordinate system (Figure 1). This procedure considers the transducer positions and their beam orientations relative to the ship, and the ship's position and motion. The following coordinate systems are used in the transformation:

S_0 is a beam coordinate system; its origin is at the centre of the transducer, with the *x*-axis in a plane normal to the beam axis and pointing starboard; the *y*-axis aligned with the beam axis, pointing downward; the *z*-axis in a plane normal to the beam axis, pointing forward;

S_1 is a transducer coordinate system; its origin is at the centre of the transducer with the *x*-axis aligned athwartship and pointing starboard; the *y*-axis is orthogonal to the transducer face, pointing downward; the *z*-axis is aligned alongship pointing forward;

S_2 is a ship coordinate system; its origin is located at a reference point on the vessel (gravity centre for example). Its *x*-axis is aligned alongship, pointing forward; its *y*-axis is aligned athwartship, pointing starboard; its *z*-axis points downward; and

S_{world} is a geographic coordinate system; its origin is the latitude and longitude of the beginning of data acquisition; its *x*-axis is in the horizontal plane, pointing north; its *y*-axis is in the horizontal plane, pointing east; its *z*-axis points downward.

For each transducer in its S_0, the observed positions of the sample $\boldsymbol{M}(x = 0, y = 0, r)$, at a range *r*, are transformed to geographic positions, $\boldsymbol{M}_{world}(x, y, z)$. For the roll and pitch stabilized ME70 data

$$\boldsymbol{M}_{world}(x,y,z) = \boldsymbol{R}_{navigation}(t) \times \boldsymbol{T}_{installation}(S_1) + \boldsymbol{R}_{yaw}(t) \times \boldsymbol{R}_{installation}(S_1) \times \boldsymbol{R}_{steering}(S_0) \times \boldsymbol{M}(0,0,r) + \boldsymbol{T}_{navigation}(t) \quad (1)$$

and for the non-stabilized EK60 data

$$\boldsymbol{M}_{world}(x,y,z) = \boldsymbol{R}_{navigation}(t) \times \begin{pmatrix} \boldsymbol{R}_{installation}(S_1) \times \boldsymbol{R}_{steering}(S_0) \times \boldsymbol{M}(0,0,r) \\ + \boldsymbol{T}_{installation}(S_1) \end{pmatrix} + \boldsymbol{T}_{navigation}(t) \quad (2)$$

where $\boldsymbol{R}_{steering}(S_0)$ is the rotation matrix for transforming S_0 to the transducer coordinate system S_1. The transformation from S_1 to a ship coordinate system S_2 requires the rotation matrix $\boldsymbol{R}_{installation}(S_1)$ and the translation matrix $\boldsymbol{T}_{installation}(S_1)$.

$\boldsymbol{R}_{navigation}(t)$ and $\boldsymbol{T}_{navigation}(t)$ are the rotation and translation matrices corresponding to the rotation and translation of S_2 to the geographic coordinate system S_{world} (Figure 1). These matrices depend on the time, *t*, of the transmission of the ping. The $\boldsymbol{R}_{navigation}(t)$ comprises three submatrices correcting for vessel heading $\boldsymbol{R}_{yaw}(t)$, pitch $\boldsymbol{R}_{pitch}(t)$, and roll $\boldsymbol{R}_{roll}(t)$:

$$\boldsymbol{R}_{navigation}(t) = \boldsymbol{R}_{yaw}(t)\boldsymbol{R}_{pitch}(t)\boldsymbol{R}_{roll}(t) \quad (3)$$

The accuracy of the transformations to S_{world} depends on the accuracy and precision of the parameters used in the transformations.

2.2. Refining sounder parameters

The beam axes of the EK60s and the ME70 are not exactly perpendicular to the transducer faces, and the transducer faces are not exactly horizontal. For the ME70, constant weights are used on the beam-formed transducer array, but its steering angles are modulated slightly by the sound speed, *c*, encountered by the transducer

during the survey. For example, for c = 1480–1510 m s^{-1}, steering angles less than 8 ° vary up to 0.1 ° (Simrad, pers. comm.). Straight-line acoustic propagation is therefore only valid for beam-steering angles < 0 ° and ranges < 200 m. In addition, account must be made for differences in the total-system time delays between echosounders. To correct for the effects of time delays and offset angles relative to the vertical in S_1, the $\boldsymbol{R}_{offset\_steering}(S_1)$ replaces $\boldsymbol{M}_{installation}(S_1)$ and the delay in range $\delta(S_0)$ is added to Equation (1) for the ME70 data

$$\boldsymbol{M}_{world}(x,y,z) = \boldsymbol{R}_{navigation}(t)\times\boldsymbol{T}_{installation}(S_1)+\boldsymbol{R}_{yaw}(b)\times\boldsymbol{R}_{offset\_steering}(S_1)\times \boldsymbol{R}_{steering}(S_0)\times\boldsymbol{M}(0,0,r+\delta(S_0))+\boldsymbol{T}_{navigation}(t) \quad (4)$$

,

and Equation (2) for the EK60 data

$$\boldsymbol{M}_{world}(x,y,z) = \boldsymbol{R}_{navigation}(t)\times\begin{pmatrix}\boldsymbol{R}_{offset\_steering}(S_1)\times\boldsymbol{R}_{steering}(S_0)\\ \times\boldsymbol{M}(0,0,r+\delta(S_0))+\boldsymbol{T}_{installation}(S_1)\end{pmatrix}+\boldsymbol{T}_{navigation}(t) \quad (5)$$

.

$\boldsymbol{R}_{offset\_steering}(S_1)$ represents the offset between the steering angle provided by the sounder manufacturer and the true steering angle, comprising misalignments of the transducer relative to the horizontal, and the beam axis relative to the normal of the transducer face.

This set of equations allows accurate location of a target detected by the EK60s and ME70 in a common geographic coordinate system. The elements of $\boldsymbol{R}_{offset\_steering}(S_0)$ and $\delta(S_0)$ can be estimated from measurements of a calibration sphere collected simultaneously by all echosounders, by minimizing differences in the transformed target position from equations (1) and (2) between echosounders (Demer *et al.*, 1999; Conti *et al.*, 2005).

Data were collected using a 25 mm diameter, tungsten-carbide sphere in the Bay of Douarnenez in 2008. The sphere was placed approximately 17 m below the transducers and 800 single-target detections of the sphere were recorded for all echosounders. Each detection included an estimate of target strength *TS*, depth *Z*, and alongship α and athwartship β angles. These data were divided into four sets of 200 detections.

To estimate $\boldsymbol{R}_{offset\_steering}(S_1)$ and $\delta(S_0)$ for each transducer, Equations (4) and (5) were inverted using the four sets of 200 *TS* measurements and a non-linear, least-squares optimization algorithm (lsqnonlin V. 4.0, Matlab, The Mathworks, USA). The average of the four parameter estimates was then calculated (Table 2).

2.3. Single-beam sampling volume

The acoustic sampling volume is the product of the equivalent beam angle (ψ) and one-half of the pulse length ($e = c\tau/2$, where c is the sound speed and τ is the pulse duration; Simmonds and MacLennan, 2005). The beams are modelled as elliptical cones with widths equal to the actual –3 dB beam widths (one-way). The modelled sampling volume is therefore an elliptical lens of thickness e and an area defined by the intersection of the cone and a sphere with a radius equal to Z.

2.4. Data selection

For this analysis, a fish school observed by an EK60 is considered if its three-dimensional shape is almost completely imaged by the ME70. For ME70 signals exceeding a threshold on volume-backscattering strength, S_v, those EK60 pings that potentially overlap with these signals, based on vessel speed and ping rate, are

tabulated. Then, for each school volume sampled by the EK60, V_{EK60}, and each tabulated ping, the degree of overlap with the school volume sampled by the ME70 V_{ME70} is computed. It is difficult to compute the intersections of multiple elliptical cones analytically; therefore, the sampling overlap is computed numerically. The V_{EK60} and V_{ME70} are gridded and their overlap is evaluated as the number of points of V_{EK60} inside V_{ME70}, divided by the total number of points in V_{ME70}. Samples overlapping less than a threshold amount, for example, 80 %, are excluded from further analysis.

2.5. Simulation

A simulation was performed to evaluate the effectiveness of the method for estimating the geometrical overlap between multiple beams, and to reduce uncertainty in measurements of the school frequency response. Datasets were simulated for shallow sardine (*Sardina pilchardus*) schools and deeper mackerel (*Scomber scombrus*) schools, using an acoustic-data simulator (OASIS; Ifremer). Each simulated dataset included data from five, single-beam echosounders (18, 38, 70, 120, and 200 kHz) and data from five, multibeam beams (103.5–118 kHz; Table 1).

The first simulated dataset comprised 60 low-density sardine schools. Alongship-school lengths varied uniformly between 13 and 30 m. School height and athwartship length were set to 0.3 times the alongship length. Athwartship school positions were randomly selected on the line from the position of the ME70 transducer at ±6 m; school depths were uniformly distributed between 20 and 40 m. All fish were assumed 21 cm long and separated by six body lengths alongship and three body lengths athwartship. This unrealistic fish density was selected as it permitted fast computation. The TS = 20log(L) – 72.6 (dB) was assumed constant for all frequencies, implying a flat frequency response; this TS vs. log-length relationship is commonly used for clupeids at 38 kHz (ICES, 1998). Therefore, each school had a mean S_v = –43.1 dB at all frequencies. A straight-line navigation course was simulated to have a speed of 10 knots and sinusoidal vessel motions (7 s periods) for pitch and roll (±2°) and yaw (±1 m). The use of a synchronized ping interval = 0.3 s ensured overlapping observations of the schools in the alongship direction.

The second simulated dataset comprised 60 mackerel schools. Their alongship lengths varied between 18 and 27 m, and again their heights and athwartship lengths were set to 0.3 times the alongship length. Athwartship school positions were randomly selected on the line from the position of the ME70 transducer at ±12 m; school depths were randomly selected between 170 and 190 m. All fish were assumed 30 cm long and spaced as described earlier for sardine. The empirical frequency-response curve for Atlantic mackerel (*Scomber scombrus*; Fernandes *et al.*, 2006) was used to extend the common 38 kHz TS vs. log-length relationship for that species (TS = 20log(L) – 84.9; Foote, 1987) to the other frequencies. Thus, each school had mean-S_v values equal to –57.5, –58, –57.5, –56.5, and –54 dB, for 18, 38, 70, 120, and 200 kHz, respectively. Vessel course, speed, and motion were the same as for the first set, but the synchronized ping interval was increased to 1 s, because of the deeper school positions.

Simulations were performed for the ideal case with all transducers identical regarding beam width, position, and beam orientation, and for the real case corresponding to the transducer specifications of RV “Thalassa” (Table 1 and Table 2). All simulated and empirical data files were stored in HAC format (ICES, 2005), which contains all the metadata necessary for application of the method.

2.6. Case study

The proposed method was applied to empirical data to study its ability to reduce uncertainty in the measurements of school frequency response. The data were collected with an ME70 and five-frequency EK60s on board RV "Thalassa" in the Bay of Biscay in 2008. Specifications for the five EK60 transducers and ME70 beams are listed in Table 1, and their relative locations on the hull of RV "Thalassa" are illustrated in Figure 2.

Data from 120 sardine schools were collected in coastal areas (school depth 15–50 m), and from 20 mackerel schools on the continental slope (school depth 170–200 m). In each case, species' identities were confirmed by trawl data. Vessel speed was 10 knots while steaming and four knots during trawling. Vessel motion was roughly the same as in the simulation study.

The data were processed with Movies+ (Berger *et al*., 2005) to identify schools observed by both the ME70 and EK60s, and to compute their mean-S_v values, s_A values, and frequency responses. For comparison, the data were also processed using the S_v thresholding technique (Korneliussen *et al*., 2008). Two thresholds were used, depending on a school's mean S_v, to calculate the frequency-response curve from the data from the centre of the schools.

3. Results

3.1. Optimization

The data collected with the sphere illustrates the effects of the steps followed to create a common coordinate system. After accounting for the differences in transducer positions and motions using Equations (1) and (2), the sphere positions remained variable (Figure 3a). By also accounting for the angle offsets and the system delays, using Equations (4) and (5), the positions became quite similar (Figure 3b).

3.2. Simulation

The combined effects of vessel movement, transducer motion, and beam width are illustrated for a simulated sardine school in S_{world} at 20 m depth (Figure 4). The significant effects of transducer positions and pitch and roll are obvious. Differences in sampling volumes are also evident between the 38 and 70 kHz data (Figure 4).

For the simulated mackerel schools, the percentage overlap between the EK60 (38 kHz) and the ME70 is displayed as an echogram (Figure 5). Some mackerel schools were not sampled adequately by the vertical echosounder, because the simulated EK60 transducer was offset in the athwartship direction relative to the simulated ME70 reference transducer. The borders of all the schools were incorrectly sampled by the EK60, resulting from the relatively wide beam widths. The shapes of the deeper mackerel schools were incorrectly observed by the EK60, because of the effects of pitch and roll. Uncertainty in school morphology and fish density observations increased with the proportion of partly overlapping echoes. The relationship was especially sensitive for schools located at the edge of the beam, stemming from slight differences in the multifrequency sampling volumes, probably because of large changes in the observed energy for each frequency.

The relative frequency responses $r(f)$, that is s_A divided by that at 38 kHz (Korneliussen and Ona, 2003), are presented for the simulated sardine datasets, both for the ideal case (identical transducers) and for the true transducer specifications, with and without application of the proposed method (Figure 6). The median estimated $r(f)$ values are presented, along with their 5th and 95th percentiles, for all schools. In the ideal case,

with all transducers identical, accurate $r(f)$ values were obtained not only with the proposed method, but also with the S_v-thresholding method (Figure 6a). In contrast, using realistic transducers, the $r(f)$ values of sardine schools distributed randomly in the athwartship direction at Z = 30 m were highly variable, resulting in wide percentile ranges (Figure 6b). For beam widths = 7 ° (e.g. 38, 70, 120, and 200 kHz EK60s), the variability in $r(f)$ values was greatest for the 70 kHz measurements, because of the athwartship offset of this transducer relative to the others. Measurements with the 18 kHz transducer (11 ° beam width) displayed substantially greater variability in $r(f)$ values than those measured using the other frequencies.
For simulated mackerel schools, mean-S_v values were strongly negatively biased for all frequencies, and for the proposed as well as the S_v thresholding method (Figure 7a). A 60 % overlap in the proposed method and thresholding at S_v = –80 dB produced similar results. An 80 % overlap produced better results than thresholding at S_v = –60 dB. Overall, the estimated $r(f)$ values were similar for both methods and close to the actual $r(f)$ values (Figure 7b), though percentile ranges were slightly wider for the proposed method.

3.3. Case study

Only approximately 15 % of the observed sardine and mackerel schools in the Bay of Biscay had greater than 80 % overlap between EK60 and ME70 observations. Empirical $r(f)$ values for the sardine and mackerel schools were similar in shape to those obtained with the simulation study, but the uncertainty was greater, especially for mackerel (Figure 8). This was probably a consequence of irregular school morphologies and school positions. Paralleling the simulation results, the proposed method with 80 % overlap and the S_v-thresholding method reduced uncertainty in $r(f)$ values (Figures 8). In contrast with the simulations for sardine, the width of the percentile intervals did not increase at 70 kHz; it was similar for all frequencies (Figure 6). For the actual mackerel schools, the uncertainty was much greater at 200 kHz than found for the simulations (Figure 7).

4. Discussion

This study proposes a method for improving estimates of $r(f)$ from single-beam echosounder data with the aid of multibeam-echosounder data, as suggested by Mayer *et al*. (2002). The proposed method accounts for misalignment between different echosounders, for beam width differences, and for transducer motion. The proposed method performs better than the S_v-thresholding method, because it exploits correlations between data simultaneously collected by different EK60s on the same platform. For shallow sardine schools and deep mackerel schools in the Bay of Biscay, the $r(f)$ values displayed a better improvement with the proposed method with 80 % overlap than using the S_v-thresholding method.
The proposed method does not require thresholding of the EK60 data, but requires thresholding of S_v for initial detections of schools in the ME70 data. Therefore, the estimated school images remain biased, even with the narrow ME70 beam widths. The overestimation of mackerel school size with the ME70 could explain the uncertainty in the measured $r(f)$ values.
The proposed method requires that the sample volume for each beam be defined. In this study, the sample volumes were, for the sake of convenience, chosen the same as those for the –3 dB beam widths. Although the sampling volume varied with S_v, it was modulated similarly for all frequencies and estimates of $r(f)$ therefore remained unchanged.

The required processing time for the proposed method depends on the amount of data and the precision of the regular grid used for computing beam overlap. Preprocessing can identify the schools to be analysed and limit the number of echoes to be considered. Depending on the desired accuracy, real-time processing with the proposed method could possibly be achieved.

Conclusion

The proposed method uses information from a calibrated, multibeam echosounder with narrow beam widths, low side lobes, and high dynamic range and measurement accuracy, namely the ME70, to reduce uncertainties in estimates of fish-school frequency response from multifrequency EK60 data. Species identification is probably improved as well, because the resulting frequency responses do not depend on the size of the schools relative to the beam widths.
The proposed method should be useful in the transition from EK60s to the ME70 for abundance estimations. Measurements made with the proposed method explain some of the differences in observations using the two systems, especially for small schools. Such insights might permit ME70 data to be used with confidence to extend EK60 time-series of abundance indices.

References

Berger, L., Durand, C., and Marchalot, C. 2007. Movies+ User Manual version 4.4. Ifremer, 72 pp.

Conti, S. G., Demer**,** D. A., Soule, M. A., and Conti, J. H. E. 2005. An improved multiple-frequency method for measuring *in-situ* target strengths. ICES Journal of Marine Science 62: 1636–1646.

Demer, D. A., Soule, M. A., and Hewitt, R. P. 1999. A multiple-frequency method for potentially improving the accuracy and precision of *in situ* target strength measurements. Journal of the Acoustical Society of America, 105 (4): 2359–2376.

Diner, N. 2001. Correction on school geometry and density: approach based on acoustic image simulation. Aquatic Living Resources, 14: 211–222.

Diner, N. 2007. Evaluating uncertainty in measurements of fish shoal aggregate backscattering cross-section caused by small shoal size relative to beamwidth. Aquatic Living Resources, 20: 117–121.

Fernandes P. G., Korneliussen R. J., Lebourges-Dhaussy A., Masse J., Iglesias M., Diner N., Ona E., Knutsen T., Gajate J., and Ponce R. 2006. The SIMFAMI Project: Species Identification Methods From Acoustic Multifrequency Information. Final report to the EC No. Q5RS–2001–02054. FRS Marine Laboratory Aberdeen, Aberdeen, UK.

Foote, K. Fish target strengths for use in echo integra**to**r surveys. 1987. Journal of the Acoustical Society of America 82:981–987.

ICES. 1998. Report of the Planning Group for Acoustic Surveys in ICES Subareas VIII and IX. 2:17. ICES Document CM 1998/G.

ICES. 2005. Description of the ICES HAC standard data exchange format, Version 1.60. ICES Cooperative Research Report 278. 86 pp.

Korneliussen, R. J., and Ona, E. 2003. Synthetic echograms generated from the relative frequency response. ICES Journal of Marine Science, 60: 636–640.

Korneliussen, R. J., Diner, N., Ona, E., Berger, L., and Fernandes, P. G. 2008. Proposals for the collection of multifrequency acoustic data. ICES Journal of Marine Science, 65: 982–994.

Massé, J. 1996. Acoustic observations in the Bay of Biscay: Schooling, vertical distribution, species assemblages and behaviour. Scientia Marina, 60 (Supplement 2): 227–234.
Mayer, L., Li, Y., and Melvin, G. 2002. 3D visualization for pelagic fisheries research and assessment. ICES Journal of Marine Science, 59: 216–225.
Simmonds, E. J., and MacLennan, D. N. 2005. Fishery Acoustics. Theory and practice. 2nd edn. Blackwell, Oxford. 437 pp.
Trenkel, V. M., Mazauric, V., and Berger, L. 2008. The new fisheries multibeam echosounder ME70: description and expected contribution to fisheries research. ICES Journal of Marine Science, 65: 645–655.

Tables

Table 1: Parameters for transducers mounted on RV “Thalassa”. These data are used for data acquisition and simulation. For the ME70, the five central beams are used.

	EK60					ME70
Frequency (kHz)	18	38	70	120	200	[103.5–118]
Beam width alongship (°)	10.6	7	6.6	7.2	6.3	[3.3;3.2;3.1;3;3.1;3.2]
Beam width athwartship (°)	10.7	7	66	7.3	6.4	[3.3;3.2;3.1;3;3.1;3.3]
Coordinates alongship (m)	27.59	27.59	26.92	26.42	26.97	26.63
Coordinates athwartship (m)	0.2	1.07	0.11	1.18	1.15	0.67
Coordinates vertical (m)	7.11	7.11	7.11	7.11	7.11	7.11
Pulse duration (μs)	1024	1024	1024	1024	1024	1024
Range resolution (m)	0.19	0.19	0.19	0.19	0.19	0.095

Table 2: Estimated offset angles and system delays for transducers installed on RV “Thalassa”.

Parameter	EK60					ME70
Frequency (kHz)	18	38	70	120	200	[103.5–118]
Offset angle alongship (°)	0.54	0.49	–0.24	–0.28	–0.60	-0.2
Offset angle athwartship (°)	-0.21	0.20	-0.22	-0.18	0.00	0.4
System delay (m) Measurements *Manufacturer’s prediction*	 –0.29 –0.29	 –0.17 –0.14	 –0.08 –0.06	 –0.03 –0.04	 –0.02 –0.02	 –0.11

Figures

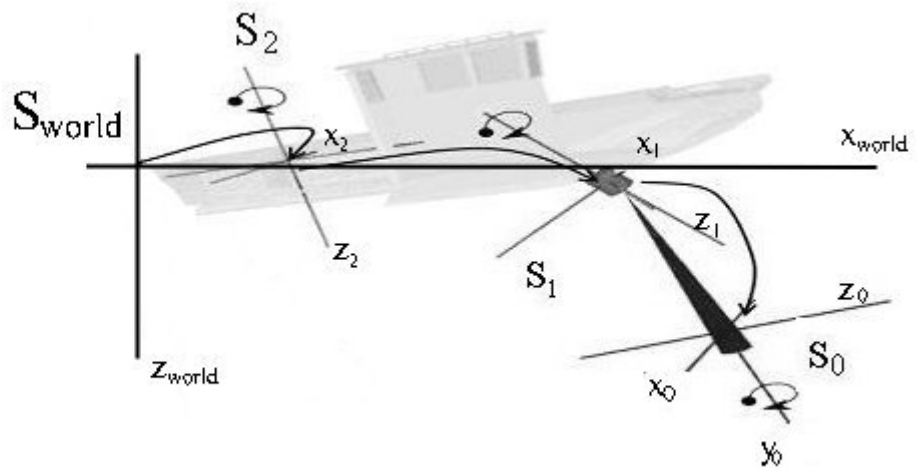

Figure 1. Definitions of the coordinate systems used for transforming the EK60 and ME70 data (see Methods for details).

Figure 2. Relative locations of the EK60 and ME70 transducers on the hull of RV “Thalassa”.

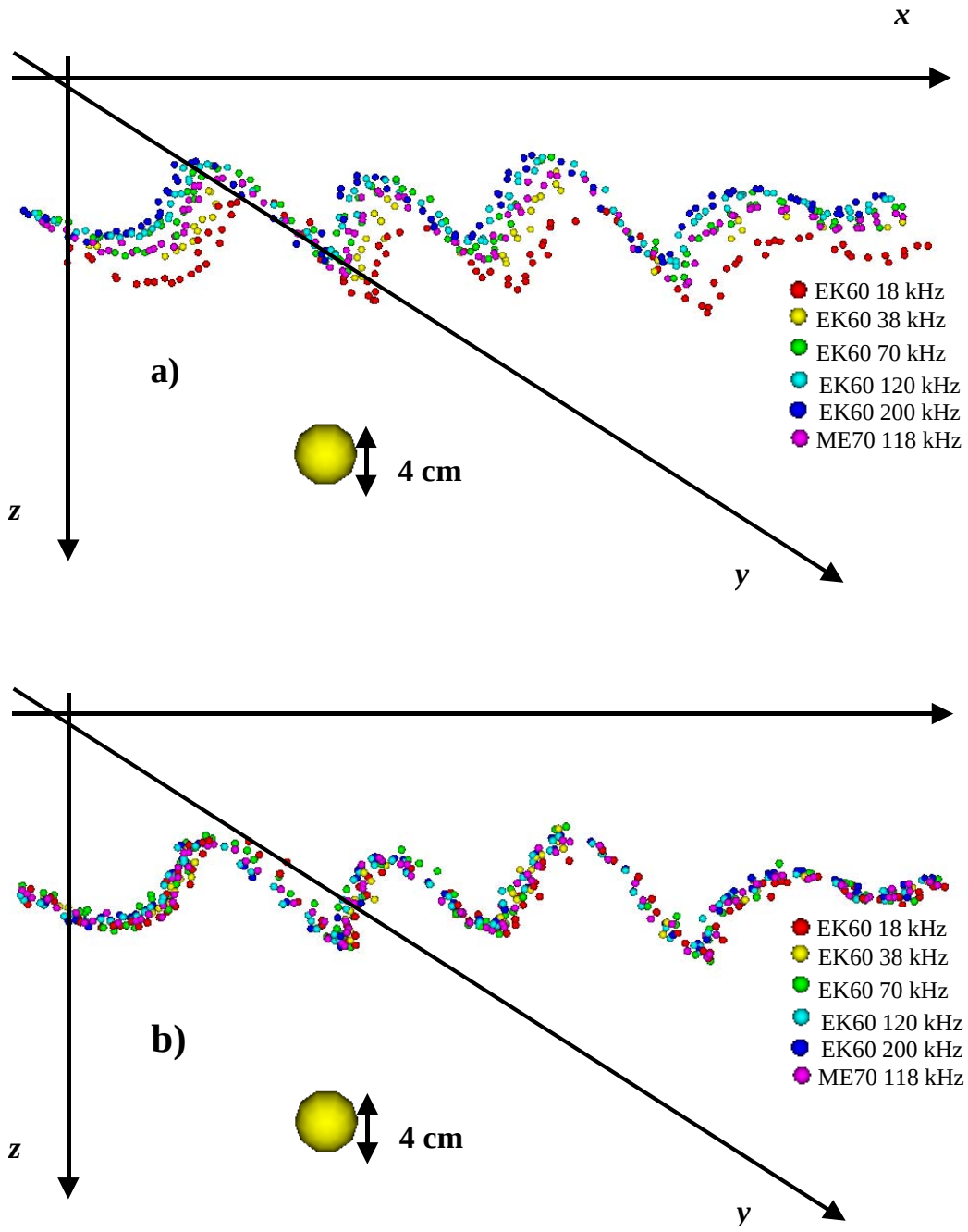

Figure 3. Effect of offset angles and system delays on sphere position in geographic coordinates. (a) Using Equations (1) and (2), which do not account for offset angles and system delays; and (b) using Equations (4) and (5), which do take these into account.

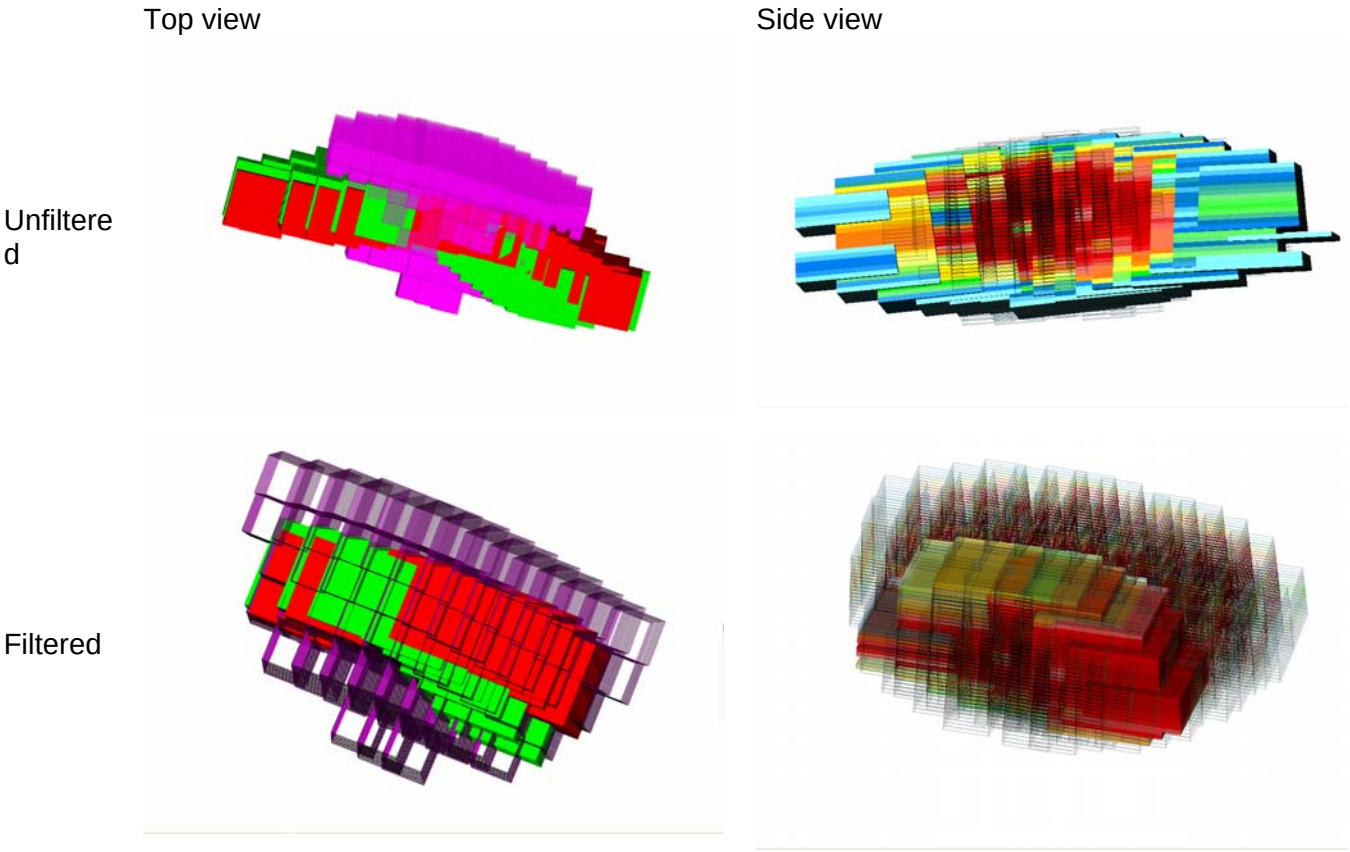

Figure 4. Simulated sardine school observed by an ME70 (magenta) and by EK60s at 38 kHz (red) and 70 kHz (green), from above (left column) and from the side (right column). In the right column, the reference echosounder (ME70) is represented in the wire frame and the 38 kHz EK60 is presented with a classical echogram colour-scale. The top view is the original data (unfiltered); the bottom view is the data restricted with to 80 % overlap (filtered).

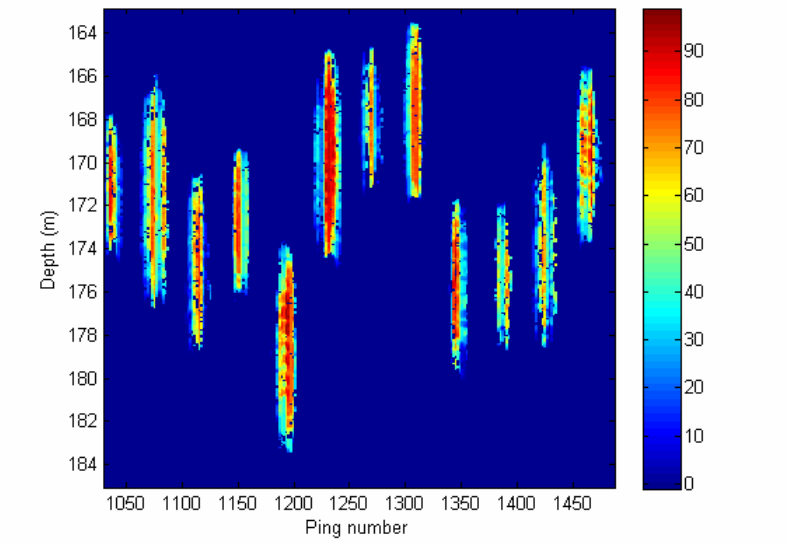

Figure 5. Echogram of the percentage of overlap for the 38 kHz EK60 with the ME70 for a simulated mackerel school.

(a) (b)

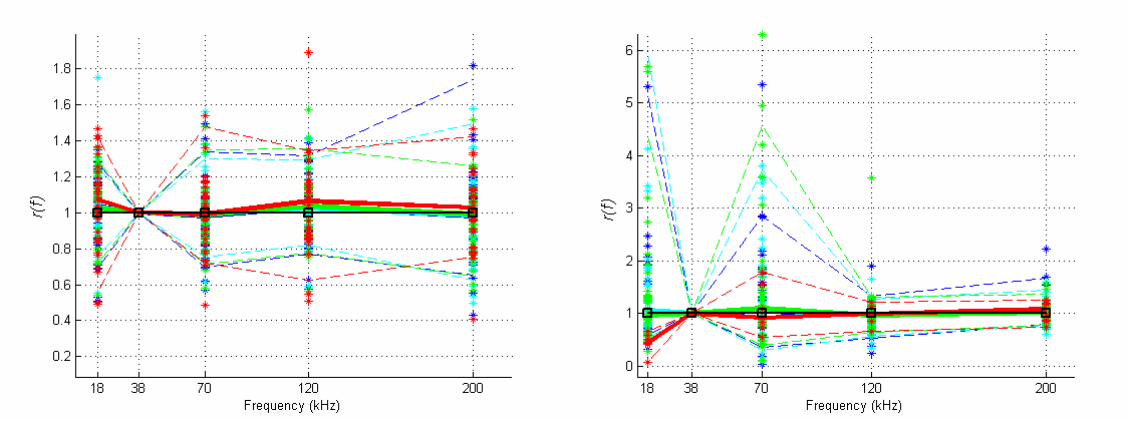

Figure 6. Simulated $r(f)$ of sardine schools at 18, 38, 70, 120, and 200 kHz, with S_v thresholds equal to –60 dB (blue), and –50 dB (cyan); and data processed with the proposed method with 60 % overlap (green) and 80 % overlap (red) between EK60 and ME70 sampled volumes. Solid lines connect median values; and dashed lines connect 5th and 95th percentiles. (a) Simulation with perfectly aligned transducers; (b) simulations assuming positions of the transducers installed on RV “Thalassa” (Figure 2).

(a) (b)

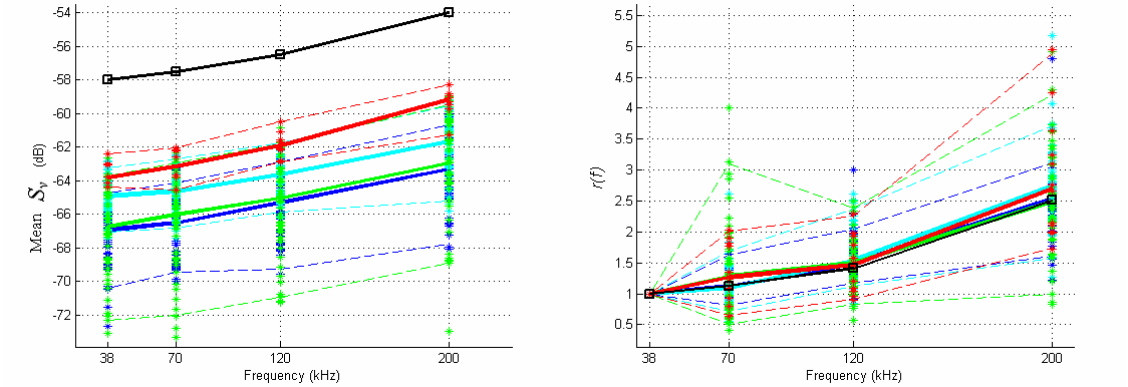

Figure 7. Mean S_v (a) and $r(f)$ (b) from simulations of schools of mackerel using the actual positioning of transducers on RV “Thalassa”, at 38, 70, 120, and 200 kHz, for S_v thresholds equal to –80 dB (blue), and –70 dB (cyan); and data processed with the proposed method with 60 % overlap (green) and 80 % overlap (red) between EK60 and ME70 sampled volumes. Solid lines connect median values; dashed lines connect 5th and 95th percentiles. For the simulations, the average true values are in black.

(a) (b)

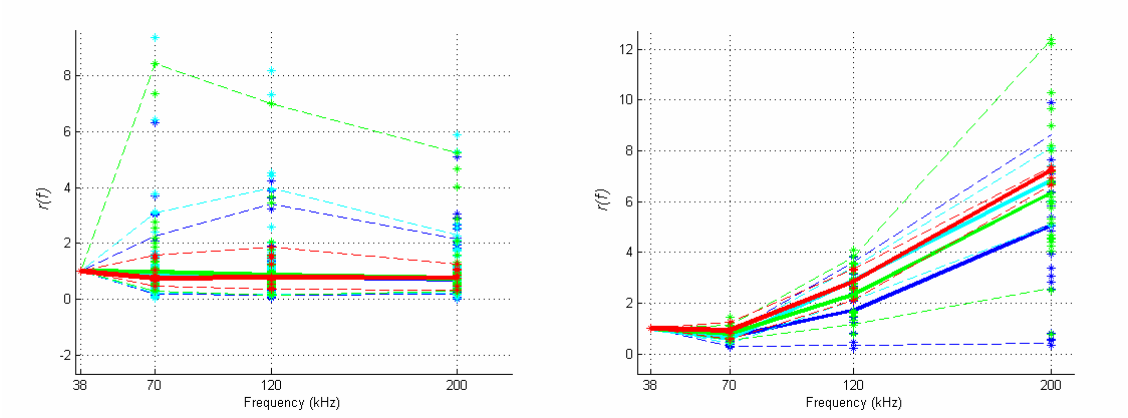

Figure 8. Empirical $r(f)$ of sardine schools (a) and mackerel (b) in the Bay of Biscay at 38, 70, 120, and 200 kHz, for S_v thresholds equal to –55 dB for sardine and –65 dB for mackerel (blue), and –50 dB for sardine and –60 dB for mackerel (cyan); and data processed with the proposed method with 60 % overlap (green) and 80 % overlap (red) between EK60 and ME70 sampled volumes. Solid lines connect median values and dashed lines connect 5th and 95th percentiles.